ATLANTIS PRESS

Advances in Intelligent Systems Research (AISR), volume 141

International Conference on Applied Mathematics, Modelling and Statistics Application (AMMSA 2017)

Treatment of Material Discontinuity in the Meshless Local Petrov-Galerkin Method

Xufei Yuan, Gendai Gu and Meiling Zhao

Department of Mathematics and Physics North China Electric Power University, Baoding 071003 China

***Abstract*—Meshless local Petrov-Galerkin (MLPG) method is presented to treat parabolic partial differential equations with discontinuous material coefficients. In this paper, we use MLPG method to solve fractional constant coefficient discontinuous media mixed boundary problem. The trial and test functions for the weak form are constructed with moving least-square interpolants in each material domain. In the proposed method, the essential boundary conditions and the jump conditions are directly imposed by substituting the corresponding terms in the system of equations. Discontinuous medium boundary condition is also applied to the solution equation. Some numerical tests are given to demonstrate the effectiveness and applicability for these problems.**

Keywords-mershless local petrov-galerkin(MLPG)method; material discontinuities; moving least squares interpolation; interface condition

I. INTRODUCTION

The MLPG method was first proposed by S.N. Atluri and T.L. Zhu [1] in 1998. It offers many advantages for analysis of both static and dynamic problems in solid mechanics. The MLPG method utilizes moving least-squares interpolants [2] which require only nodes, unencumbered by elements and elemental connectivity, to construct the shape functions.

In the twentieth century, the finite element method, which combines the Ritz-Galerkin method and the element-based slice polynomial interpolation approximation, opens up a new era of numerical computation, which deeply affects the branches of engineering physics. In the field of electrical engineering, since the introduction of Winslow for the first time in 1965, the finite element method has been widely applied and developed rapidly. Then mesh-less method followed finite element method and developed rapidly. It has become one of the main numerical methods for quantitative analysis and optimization of electromagnetic and electromagnetic wave problems. The main advantage of this approach is that it does not require a "grid", either for interpolation or for integration purposes. The essential boundary conditions and the jump conditions are directly imposed by substituting the corresponding terms in the system of equations. Although there is a great advantage in using MLPG, there are some drawbacks in implementing this method. For example, the nature of complex non-polynomial shape functions can lead to larger costs in implementing numerical integration schemes.

The purpose of this paper is to improve the weight function in the MLS approximation and add the interface condition processing to the mesh-less method. We can get a very effective mesh-less method for solving two-dimensional mechanical problems that contain material discontinuities.

In the article we use MLPG method to solve the following problems:

$$\Omega : -\nabla \cdot (\gamma(\mathbf{x})\nabla\varphi(\mathbf{x})) = f(\mathbf{x}) \tag{1}$$

$$\Gamma_d : \varphi(\mathbf{x}) = g(\mathbf{x}), \tag{2}$$

where, $g(\mathbf{x}) \in H^{1/2}(\partial\Omega)$,

$$\gamma(\mathbf{x}) = \begin{cases} k_1 & \mathbf{x} \in \Omega_1 \\ k_2 & \mathbf{x} \in \Omega_2 \end{cases}. \tag{3}$$

Easy to analyze, we assume that when $\mathbf{x} \in \Omega_i, (i = 1,2)$

$\varphi_i(\mathbf{x}) = \varphi(x_i, y_i)$. (1)-(3) can be written in the following form:

$$-k_i \Delta\varphi_i(\mathbf{x}) = f(\mathbf{x}), \mathbf{x} \in \Omega_i, i = 1,2, \tag{4}$$

$$\varphi_1(\mathbf{x}) - \varphi_2(\mathbf{x}) = 0, \mathbf{x} \in \Gamma_\tau \tag{5}$$

$$n_1 \cdot k_1 \nabla\varphi_1(\mathbf{x}) + n_2 \cdot k_2 \nabla\varphi_2(\mathbf{x}) = j(\mathbf{x}), \mathbf{x} \in \Gamma_\tau \tag{6}$$

$$\varphi_1(\mathbf{x}) = g(\mathbf{x}), \mathbf{x} \in \partial\Omega_i \cap \partial\Omega \tag{7}$$

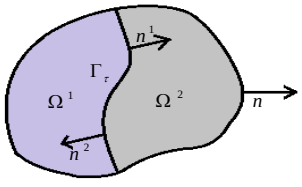

FIGURE I. TWO-DIMENSIONAL NON-HOMOGENEOUS MEDIA MODEL

where n_i is Unit outside the normal of $\Omega_i, (i = 1,2)$.

where $\mathbf{x}=[x,y], k_i(i=1,2)$ is constant. Γ_d is Dirichlet boundary. On which apply function $g(\mathbf{x})$. Γ_τ is discontinuous media boundary. In three dimensions, $\mathbf{x}[x,y,z]$, the border is a closed face, Γ_τ is the discontinuous medium interface.

II. MATHEMATICAL FORMULATION

A. *The Shape Function of MLPG*

The approximation function of mesh-less local Petro-Galerkin method (MLPG) is constructed by moving least squares (MLS) approximation.

Consider a sub-domain Ω_s, the neighborhood of a point $\mathbf{x}$ and denoted as the domain of definition of the MLS approximation for the trial function at $\mathbf{x}$, which is located in the problem domain Ω_s. To approximate the distribution of function u in Ω_s, over a number of randomly located nodes $\mathbf{x}_i, i=1,2,\ldots,n$ the moving least square approximation $u^h(\mathbf{x})$ of $\varphi(\mathbf{x})$, $\forall\mathbf{x}\in\Omega_s$ can be defined by

$$u^h(\mathbf{x})=\mathbf{P}^T(\mathbf{x})a(\mathbf{x}),\forall\mathbf{x} \tag{8}$$

where $\mathbf{P}^T(\mathbf{x})=[p_1(\mathbf{x}),p_2(\mathbf{x}),\ldots,p_m(\mathbf{x})]$ is the complete monomial of order m ; and $a(\mathbf{x})$ is a vector containing coefficients $a_j(\mathbf{x}), j=1,2,\ldots,m$, which are functions of the space coordinates $\mathbf{x}$.

Discrete form is as follows:

$$u_i^h(\mathbf{x})=\sum_j^m p_j(\mathbf{x})a_{ij}(\mathbf{x})=\mathbf{P}^T(\mathbf{x})a_i(\mathbf{x}),\forall\mathbf{x} \tag{9}$$

A linear basis $(m=3)$ in a two-dimensional domain is applied in this paper and is given by

$$\mathbf{p}^T(\mathbf{x})=[1,x,y] \tag{10}$$

The coefficients $a_i(\mathbf{x})$ are obtained at any point $\mathbf{x}$ by stationarity of a weighted, discrete L_2 norm as follows:

$$\mathbf{J}=\sum_I^n\sum_j^m w_I(\mathbf{x})[p_I(\mathbf{x}_I)a_{ij}(\mathbf{x})-\mathbf{u}_{iI}]^2 \tag{11}$$

Where $w_I(\mathbf{x})=w(\mathbf{x}-\mathbf{x}_I)\neq 0$ is weight function, $\mathbf{u}_{iI}=\varphi(\mathbf{x})$ are the coefficients associated with node I at $\mathbf{x}=\mathbf{x}_I$,and n is the number of nodes in the neighborhood of $\mathbf{x}$. The neighbor points of the $\mathbf{x}$ are determined by the radius of the affected domain at that point, d_{mi}. If $\mathbf{x}$ falls in the influence domain of the node $\mathbf{x}_I$, then the node $\mathbf{x}$ influences $\mathbf{x}_I$ and is considered to be a neighbor node.

The stationarity of $J(\partial J/\partial a_{ij}(\mathbf{x}))=0$ leads to the following linear relationship.

$$\mathbf{A}(\mathbf{x})a_i(\mathbf{x})=\mathbf{B}(\mathbf{x})\mathbf{u}_{iI} \tag{12}$$

where the matrices $\mathbf{A}(\mathbf{x})$ and $\mathbf{B}(\mathbf{x})$ are defined as:

$$\mathbf{A}(\mathbf{x})=\sum_I^n w_I(\mathbf{x})\mathbf{p}(\mathbf{x}_I)\mathbf{p}^T(\mathbf{x}_I) \tag{13}$$

$$\mathbf{B}(\mathbf{x})=[w_1(\mathbf{x})\mathbf{p}(\mathbf{x}_1),w_2(\mathbf{x})\mathbf{p}(\mathbf{x}_2),\ldots,w_n(\mathbf{x})\mathbf{p}(\mathbf{x}_n)] \tag{14}$$

And the node coefficient vector is given by the following equation:

$$\mathbf{u}_{iI}=[\varphi_{i1},\varphi_{i2},\ldots,\varphi_{in}] \tag{15}$$

Solving $a(\mathbf{x})$ from (12) and substituting it into (9), the MLS interpolant of $\varphi(\mathbf{x})$ may now be written as:

$$u_i^h(\mathbf{x})=\sum_I^n\sum_j^m p_j(\mathbf{x})[\mathbf{A}^{-1}(\mathbf{x}_I)\mathbf{B}(\mathbf{x})]_{jI}\mathbf{u}_{iI}=\sum_I^n\phi_I\mathbf{u}_{iI} \tag{16}$$

where the shape function $\phi_I(\mathbf{x})$ is defined

$$\phi_I(\mathbf{x})=\sum_j^m p_j(\mathbf{x})[\mathbf{A}^{-1}(\mathbf{x})\mathbf{B}(\mathbf{x})]_{jI}=\mathbf{p}^T(\mathbf{x})\mathbf{A}^{-1}(\mathbf{x})\mathbf{B}(\mathbf{x}) \tag{17}$$

B. *The Selection of the Weight Function*

(1)The choice of weight function in the mesh-less method is critical. In this paper we use Quadratic spline function and gauss weight function:

$$w(\bar{d})=\begin{cases}1-6\bar{d}^2+8\bar{d}^3-3\bar{d}^4 & \bar{d}\le 1\\ 0 & \bar{d}>1\end{cases},$$

$$w(d_I)=\begin{cases}\dfrac{\exp[-(d_I/c_I)^{2k}]-\exp[-(r_I/c_I)^{2k}]}{1-\exp[-(r_I/c_I)^{2k}]} & d_I\le r_I\\ 0 & d_I>r_I\end{cases}$$

In those weight functions, $d_I=\|\mathbf{x}-\mathbf{x}_I\|$ is the distance of $\mathbf{x}$ to $\mathbf{x}_I$; r is the influence radius of point $\mathbf{x}$; $\bar{d}=d_I/r$.

c, c_I and k are control variables, which control the shape of the weight function.

C. Local Weak Formulation

Consider the following weak form in Ω_s associated with (1)

$$\int_{\Omega_s}(\nabla\cdot(\gamma(\mathbf{x})\nabla\varphi(\mathbf{x}))+f)v d\Omega-\alpha\int_{\Gamma_d}(\varphi(\mathbf{x})-g(\mathbf{x}))v ds=0 \quad (18)$$

Where v is a test function. Using the divergence theorem and integral subsection integration yields the following expression:

$$\begin{aligned}&\int_{\Omega_s}\gamma(\mathrm{x})\nabla\varphi(\mathrm{x})\cdot\nabla v d\Omega-\int_{\partial\Omega_s/\tau}\gamma(\mathrm{x})\frac{\partial\varphi(\mathrm{x})}{\partial n}v ds-\int_{\tau}\gamma(\mathrm{x})\frac{\partial\varphi(\mathrm{x})}{\partial n}v ds \\ &+\alpha\int_{\Gamma_d}\varphi(\mathrm{x})v ds=\int_{\Omega_s}f v d\Omega+\alpha\int_{\Gamma_d}g(\mathrm{x})v ds\end{aligned} \quad (19)$$

The function $\varphi(\mathbf{x})$ and coefficients $\gamma(\mathbf{x})$ can be also discontinuous across the interface τ, i.e.

$$\varphi(\mathbf{x})=\begin{cases}\varphi_1(\mathbf{x}) & \mathbf{x}\in\Omega_1\\ \varphi_2(\mathbf{x}) & \mathbf{x}\in\Omega_2\end{cases},\gamma(\mathbf{x})=\begin{cases}k_1 & \mathbf{x}\in\Omega_1\\ k_2 & \mathbf{x}\in\Omega_2\end{cases}.$$

In order to satisfy the condition(5)-(6) for the discontinuous boundary, decompose Γ_τ into overlapping $\Gamma_{\tau_{\Omega^1}}$ and $\Gamma_{\tau_{\Omega^2}}$. In Figure 2, the point on $\Gamma_{\tau_{\Omega^1}}$ is affected only by the nodes on Ω^1 and Γ_τ, and the point on $\Gamma_{\tau_{\Omega^2}}$ is affected only by the nodes on Ω^2 and Γ_τ.

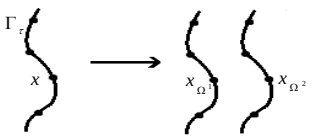

FIGURE II. EQUIVALENT TREATMENT OF DISCONTINUOUS BOUNDARY Γ_τ

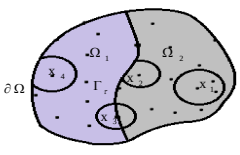

FIGURE III. THE INFLUENCE DOMAIN OF THE DISCRETE POINTS NEAR Γ_τ

In figure 3, the impact domain of all nodes can not cross the media interface, so the point in each medium is only affected by the nodes in the medium region and the nodes on Γ_s.

To find a weak formulation for the above interface problem, we multiply (1), (5) and (6) by test function v and integrate on both sub-regions Ω^1 and Ω^2. Applying Green's theorem in the domain Ω^1, outside of the interface τ, we get the interface condition:

$$\begin{aligned}&\int_{\Omega_s}k_1\nabla\varphi(\mathbf{x})\cdot\nabla v d\Omega-\int_{\partial\Omega_s^1/\tau}k_1\frac{\partial\varphi(\mathbf{x})^1}{\partial n^1}v ds-\int_{\tau}k_1\frac{\partial\varphi(\mathbf{x})}{\partial n}v ds \\ &+\alpha\int_{\Gamma_d}\varphi(\mathbf{x})v ds=\int_{\Omega_s}f v d\Omega+\alpha\int_{\Gamma_d}g(\mathbf{x})v ds\end{aligned} \quad (20)$$

Similarly, we have the following relation from the inside of the interface, i.e., Ω^2

$$\begin{aligned}&\int_{\Omega_s}k_2\nabla\varphi(\mathbf{x})\cdot\nabla v d\Omega-\int_{\partial\Omega_s^2/\tau}k_1\frac{\partial\varphi(\mathbf{x})^2}{\partial n^2}v ds-\int_{\tau}k_2\frac{\partial\varphi(\mathbf{x})}{\partial n}v ds \\ &+\alpha\int_{\Gamma_d}\varphi(\mathbf{x})v ds=\int_{\Omega_s}f v d\Omega+\alpha\int_{\Gamma_d}g(\mathbf{x})v ds\end{aligned} \quad (21)$$

Since $\mathbf{n}_\tau^1=-\mathbf{n}_\tau^2=\mathbf{n}_\tau$ adding (16) and (17) together, we get

$$\begin{aligned}&\sum_{s=1}^{n}(\int_{\Omega_s}\gamma(\mathrm{x})\nabla\varphi(\mathrm{x})\cdot\nabla v d\Omega-\int_{\partial\Omega_s/\tau}\gamma(\mathrm{x})\frac{\partial\varphi(\mathrm{x})}{\partial n}v ds+\alpha\int_{\Gamma_d}\varphi(\mathrm{x})v ds) \\ &=\sum_{s=1}^{n}(\int_{\Omega_s}f v d\Omega+\alpha\int_{\Gamma_d}g(\mathrm{x})v ds+\int_{\tau}j(\mathrm{x})v ds).\end{aligned} \quad (22)$$

Consider (22), (17) we get integral equation satisfied (4)-(7) in Ω (n is the number of Ω_s):

$$\begin{aligned}K_{IJ}&=\int_{\Omega_s}\gamma(\mathrm{x})(\phi_{J,x}(\mathrm{x})v_{,x}(\mathrm{x},\mathrm{x}_I)+\phi_{J,y}(\mathrm{x})v_{,y}(\mathrm{x},\mathrm{x}_I))d\Omega \\ &-\int_{\partial\Omega_s/\tau}\gamma(\mathrm{x})\frac{\partial\phi_J(\mathrm{x})}{\partial n}v(\mathrm{x},\mathrm{x}_I)ds+\alpha\int_{\Gamma_d}\phi_J(\mathrm{x})v(\mathrm{x},\mathrm{x}_I)ds \\ f_I&=\int_{\Omega_s}f v(\mathrm{x},\mathrm{x}_I)d\Omega+\alpha\int_{\Gamma_d}g(\mathrm{x})v(\mathrm{x},\mathrm{x}_I)ds+\int_{\tau}j(\mathrm{x})v(\mathrm{x},\mathrm{x}_I)ds.\end{aligned} \quad (23)$$

$I=1,2,\ldots N, J=1,2,\ldots,M$. N is the number of nodes in Ω, M is the number of nodes in Ω_s.

Finally, we obtain the linear system $K\mathbf{u}=f$ where each node corresponds to a row of the matrix K. It should be noted that for each point of interface, two components of the unknown vector $\mathbf{u}$ and two rows of the matrix K are considered. In the MLPG method by employing MLS approximation, we want to find good estimates for the target

function $\phi_I(\mathbf{x})$ in terms of the values at nodes, to set up the matrix K.

III. NUMERICAL EXPERIMENTS

Example 1

In this section consider two numerical examples. We show the effectiveness of MLPG algorithm to solve the discontinuous media problem by comparing the error.

In figure 4, $\Omega=[0,1]\times[0,1]$, $\Omega=\Omega_1\cup\Omega_2$, $\Omega_1=[0,0.5]\times[0,1]$, $\Omega_2=[0.5,1]\times[0,1]$.

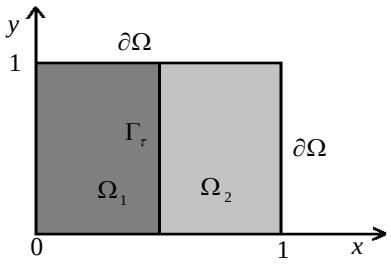

FIGURE IV. TWO REGIONS OF DIFFERENT MEDIA

Given $\varphi_1(\mathbf{x})$ and $\varphi_2(\mathbf{x})$ that satisfy (1)-(2):

$$\varphi_1(\mathbf{x})=(\frac{k_2 ax}{k_1}+(\frac{1}{2}-\frac{k_2}{2k_1})a+b)y\,, \tag{24}$$

$$\varphi_2(\mathbf{x})=(ax+b)y\,, \tag{25}$$

$$k_1=1,k_2=20\,,\ a=1,b=5\,,$$

here we consider the impact of the node number and the weight function on error. First, define the norm of the error within Ω in following:

$$e_M(\Omega)=\max|u_{i,j}^h-\varphi(x_i,y_j)|$$

$u_{i,j}^h$ is numerical solution on (x_i,y_j).

TABLE I. TABLE OF ERROR AND RATE WHEN H IS DIFFERENT

h	$e_M^1\times10^{-3}$	rate	$e_M^2\times10^{-3}$	rate
0.1000	19.7	0.16	16.6	0.23
0.0667	15.8	0.30	13.8	0.41
0.0500	12.3	0.69	10.0	0.85
0.0250	8.3	1.27	6.5	1.37
0.0200	7.0	1.38	5.9	1.50
0.0167	6.9	1.95	5.3	2.05

In the table, e_M^1 is the norm $e_M(\Omega)$ when weight function v is quadratic spline function, e_M^2 is the norm $e_M(\Omega)$ when weight function v is gauss weight function. In the following we select two error surface map (when h=0.1 and h=0.0167) for comparing.

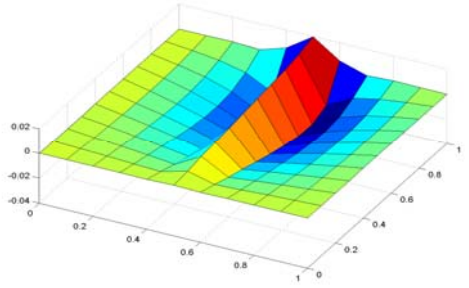

FIGURE V. THE ERROR OBTAINED WHEN H=0.1

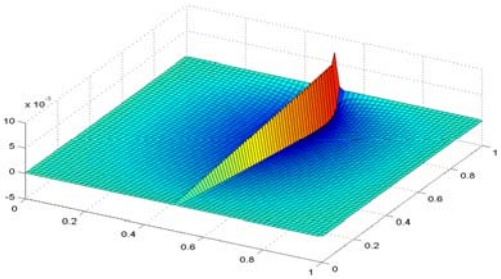

FIGURE VI. THE ERROR OBTAINED WHEN H=0.0167

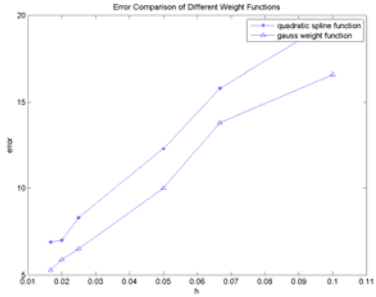

FIGURE VII. ERROR COMPARISON CHART

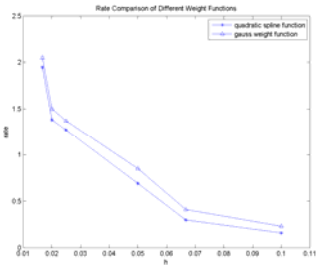

FIGURE VIII. RATE COMPARISON CHART

Example 2

We consider the domain $\Omega = [0,3] \times [0,3]$, divided into one interior domain, $\Omega_1 = (1,2) \times (0.5,1.5)$, and one exterior $\Omega_2 = \Omega / \Omega_1$, we set $k_1 = k_2 = 1$.

$$f = \frac{2\pi^2}{9} \sin(\pi x / 3) \sin(\pi y / 3) \tag{26}$$

$$\varphi = \sin(\pi x / 3) \sin(\pi y / 3) \tag{27}$$

TABLE II. TABLE OF ERROR AND RATE WHEN H IS DIFFERENT

h	$e_M^1 \times 10^{-3}$	rate	$e_M^2 \times 10^{-3}$	rate
0.250	8.9	0.30	7.4	0.31
0.200	8.5	0.45	6.6	0.51
0.150	5.3	0.68	4.8	0.75
0.075	3.3	1.14	3.0	1.56
0.050	2.7	1.50	2.1	1.63

In the following we select two error map for comparing.

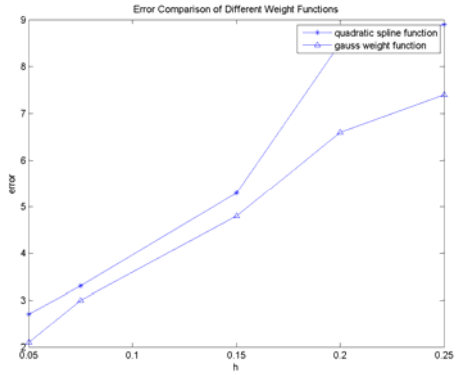

FIGURE IX. ERROR COMPARISON CHART

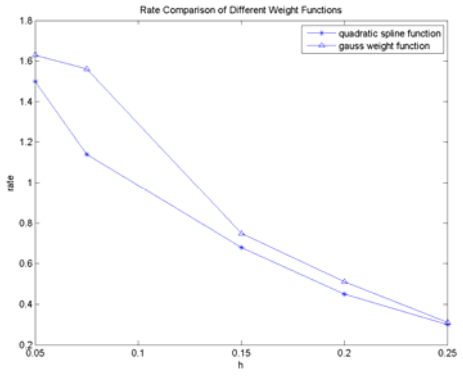

FIGURE X. RATE COMPARISON CHART

IV. CONCLUDING REMARKS

In this paper, we use MLS approximate function and implement further processing of interface nodes, to achieve an efficient and fast solution to the equation. In addition, through numerical experiments we get a conclusion: In that question, gauss weight function is better than quadratic spline function as weight function. With the increase in the number of nodes the error is getting smaller.

ACKNOWLEDGMENT

The work was supported by the National Natural Science Foundation of China (No.11401208) and Natural Science Foundation of Hebei Province (No. A2016502001).

REFERENCES

[1] S.N. Atluri, T.L. Zhu "A new meshless local Petrov–Galerkin(MLPG) approach in computational mechanics".Springer J. Comput. Mech.1998, pp. 117–127.

[2] P. Lancaster, K. Salkauskas "Surfaces generated by moving least squares methods," J. Math. Comput. 1981 pp. 141-158.

[3] S.R. Beissel "Nodal integration of the Element-Free Galerkin method and related topics in the stability of computational mechanics, " Ph.D. Thesis, Northwestern University, 1994.

[4] S.M. Hosseini, J. Sladek, V. Sladek "Two dimensional analysis of coupled non-Fick diffusion-elastodynamics problems in functionally graded materials using meshless local Petrov–Galerkin (MLPG) method," C. Appl. Mech. Engrg, 2015, pp. 937-946.

[5] J. Sladek, V. Sladek, S. Krahulec, C.H. Zhang, "Interface crack problems in anisotropic solids analyzed by the MLPG," CMES Comput. Model. Eng. Sci. 2009 pp. 223–252.

[6] L. Mu, J. Wang, G. Wei, X. Ye, S. Zhao, "Weak Galerkin methods for second order elliptic interface problems," J. Comput. Phys. 2013 pp. 106–125.

[7] S.N. Atluri, T.L. Zhu "The meshless local Petrov–Galerkin (MLPG) approach for solving problems in elasto-statics," Springer J Comput. Mech, 2000. vol 25, pp. 169–179.

[8] R. Yang, L. Tao "Mechanical quadrature methods and their extrapolations for solving boundary integral equations of the conductivity problem with discontinuous media," Elsevier J. Engrg Analy Bound Ele, 2008, pp. 176-185.

[9] R.W. Cordes "Treatment of material discontinuity in the Element-Free Galerkin method" Elsevier J. Comput. Methods Appl. Mech. Engrg. 1996, pp. 75-89

[10] Y.Y. Lu, T. Belytschko, L. Gu " A new implementation of the Element Free Galerkin method," J. Comput. Methods Appl. Mech. Engrg. 1994, pp. 227-286.

[11] T. Techapirom, A. Luadsong, "The MLPG with improved weight function for two-dimensional heat equation with non-local boundary condition," J. Elsevier, 2013, pp. 341–348.

[12] P. Hansbo , C. Lovadina , I Perugia , G Sangalli, "A Lagrange multiplier method for the finite element solution of elliptic interface problems using non-matching meshes," Springer J. Num math 2005, pp.91-115.

[13] C.T. Wu, Z. Li, M.C. Lai, "Adaptive mesh refinement for elliptic interface problems using the non-conforming immersed finite element method, "Int. J. Numer. Anal. Model. 2011 pp. 466–483.

[14] D. Wang, Y. Sun, L. Li, "A discontinuous Galerkin meshfree modeling of material interface," CMES Comput. Model. Eng. Sci. 2009 pp. 57–82.

[15] Zhao M, Nie Y. "A study of boundary conditions in the meshless local Petrov-Galerkin (MLPG) method for electromagnetic field computations" [J]. Computer Modeling in Engineering & Sciences, 2008, 37(2):97-112.